Chapter 2.8

An overview of regression methods in hyperspectral and multispectral imaging

Irina Torres[a] and José Manuel Amigo[b,*]
[a]*Department of Bromatology and Food Technology, University of Córdoba, Campus of Rabanales, Córdoba, Spain;* [b]*Professor, Ikerbasque, Basque Foundation for Science; Department of Analytical Chemistry, University of the Basque Country, Spain; Chemometrics and Analytical Technologies, Department of Food Science, University of Copenhagen, Denmark*
**Corresponding author.*

1. Introduction

One of the major applications of hyperspectral imaging (HSI) and multispectral imaging (MSI) is the segmentation and/or classification of the constituents of the measured surface [1]. Nevertheless, the quantitation of the constituents of a sample is of outmost importance in fields such as food research and pharmaceutical production (among others) [2–5], which is made possible by multivariate regression methods. Multivariate regression methods [6–9] are those in which the correlation between a set of $\mathbf{X}$ ($M \times \lambda$) with M independent samples measured at λ independent variables, and a predictor/dependent variable $\mathbf{y}$ ($M \times 1$) is calculated as:

$$\mathbf{y} = \mathbf{Xb} + \mathbf{b}_0 + \mathbf{e} \tag{1}$$

where $\mathbf{b}$ ($\lambda \times 1$) is known as the regression vector, $\mathbf{b_0}$ is the intercept coefficient, and $\mathbf{e}$ is the error vector.

In the context of HSI and MSI, the classical approach of multivariate regression methods in single-point spectroscopy is normally adopted, in such a way that $\mathbf{X}$ is a set of M pixels selected from samples where the value of the corresponding $\mathbf{y}$ is perfectly known (calibration set). The spectra are recorded measuring in λ

Hyperspectral Imaging. https://doi.org/10.1016/B978-0-444-63977-6.00010-9

wavelengths. Consequently, **b** will be a vector that contains as many rows as λ. If there are more than 1 **y** predictor variables, Eq. (1) expands as:

$$\mathbf{Y} = \mathbf{XB} + \mathbf{B}_0 + \mathbf{E} \tag{2}$$

Although there are many ways of solving the problem postulated in the previous equations, the classical ones are the so-called linear models, like ordinary least squares/multilinear regression (OLS/MLR), principal component regression, and partial least squares (PLS). Moreover, nowadays there is a trend to use the denominated nonlinear models (e.g., artificial neural networks, ANN), as well as models mixture between linear and nonlinear approaches, like the support vector machine (SVM).

Despite the fact that the usefulness demonstrated by the regression methods in determining the exact concentration in each individual pixel or in the bulk sample measured, and the high amount of published research in different matrices, there is still a lack of knowledge about the implication of constructing a regression method using spectra and predicting the compound in the entire surface in a pixel-wise manner. In this chapter, we will review the basics in the theoretical background of linear methodologies. Furthermore, the essential steps for understanding the fundamentals behind the most common linear regression methods will be highlighted, providing the key references for a deeper knowledge [10]. We will also review the most relevant applications based on the food and pharmaceutical production frameworks, paying special attention on remarking important guidelines for applying regression models in HSI and MSI.

2. Brief theory of most popular regression methods

2.1 Multiple linear regression

Multiple linear regression (MLR) [11], also known as ordinary least squares (OLS), is the simplest way of calculating the regression vector between a set of independent measurements **X** and a dependent variable. The regression vector **b** is calculated as follow:

$$\mathbf{b_{OLS}} = (\mathbf{X}'\mathbf{X})^{-1}\mathbf{X}'\mathbf{y} \tag{3}$$

Alternatively, if there are more than one dependent variable:

$$\mathbf{B_{OLS}} = (\mathbf{X}'\mathbf{X})^{-1}\mathbf{X}'\mathbf{Y} \tag{4}$$

The simplicity of this regression method is the main feature of it, even when weights are applied to the variables to minimize the noise and increase the importance of some of them. Nevertheless, a big problem of MLR is the existence of colinearity between variables. Therefore, a good variable selection step might be strongly advised.

2.2 Principal component regression

In order to avoid the problem of noninformative and colinear variables, a principal component model (PCA) can be performed on **X** as the first step.

Then, the regression vector(s) will be calculated by using the scores obtained in that PCA model:

$$1)\ \mathbf{X} = \mathbf{TP}^{\mathbf{T}} + \mathbf{E} \tag{5}$$

$$2)\ \mathbf{B}_{\mathbf{OLS,PCR}} = (\mathbf{T}'\mathbf{T})^{-1}\mathbf{T}'\mathbf{Y} \tag{6}$$

Therefore,

$$\mathbf{3)}\ \mathbf{B}_{\mathbf{PCR}} = \mathbf{PB}_{\mathbf{OLS,PCR}} \tag{7}$$

This methodology, called principal component regression (PCR) [12], has the benefit and, at the same time, the drawback of using the scores information coming from the independent matrix. It is a benefit because the scores contain only the relevant noncolinear information of **X**. The main issue comes with the fact that PCA only considers the variance of **X**, without looking at the covariance between **X** and **Y**. Therefore, important information related to **Y** could be left in the residuals of the PCA models if there is not a proper choice of the number of principal components.

2.3 Partial least squares

PLS [13] appeared to overcome the limitations of the previous methods, considering both the variance of **X** and the covariance between **X** and **Y**. Now, PLS projects **X** and **Y** in a new space:

$$\mathbf{X} = \mathbf{TP}^{\mathbf{T}} + \mathbf{E}_{\mathbf{X}} \tag{8}$$

$$\mathbf{Y} = \mathbf{UQ}^{\mathbf{T}} + \mathbf{E}_{\mathbf{Y}} \tag{9}$$

where **U** and **Q** are the scores and loadings, respectively, of **Y**. The projections shown in the equations above are done simultaneously by maximizing the correlation between the scores **T** and **Q**:

$$\mathbf{U} = \mathbf{RT} \tag{10}$$

Then the regression vector can be calculated as it is shown in Eq. (2). Normally, when **Y** is a column vector (i.e., there is only one dependent variable) the model is denoted as PLS1; while if **Y** contains more than one column vector the model is denoted as PLS2. PLS is, arguably, the most widely used method for multivariate regression, with many different algorithms for its calculation [14].

2.4 Some notes about support vector regression and artificial neural networks

As the reader could see, just a short space is dedicated to define support vector regression (SVR) and artificial neural networks in regression (ANN-R). Most

of the applications of SVR and ANN-R in HSI and MSI are focused on classification issues, and they will be covered in different chapters. Nevertheless, as they have also been used in regression context, it is important to highlight some aspects herein. In the regression (quantitation) context, most of the data that we deal with HSI and MSI have a linear nature. In most cases, the images are acquired using near-infrared (NIR) and visible (VIS) spectral range, being two regions ruled by the well-known Beer–Lambert Law. Therefore, it could be considered that the response to any compound will be linear. Acknowledging that there might be artifacts (e.g., shadows) that can compromise the linearity of the signal, and even though there are some data preprocessing methods that can correct or minimize those deviations [15,16], there are some situations in which SVR and ANN-R are more adequate to quantify compounds in surfaces.

SVR is an extension of the well-known SVM algorithm [17] applied in multivariate regression problems. As SVM, the SVR contains the main features that characterize the maximum margin algorithm [18,19]. Nevertheless, there are important differences with respect to SVM that must be considered. SVR looks for a feasible solution by individualizing the hyperplane that maximizes the margin. Nevertheless, since the final solution is a real number that needs to be predicted, the tolerance of the error is more flexible. On the contrary to what it can be thought, SVR can be performed in a linear or nonlinear manner, depending on what is known as the "kernel-trick." ANN [20] can be defined as a nonlinear computational tool, with more or less computational complexity, that aims as stablishing a nonlinear correlation between **X** and **Y**. ANN are usually built to deal with highly nonlinear problems, where traditional linear models fail.

3. Considerations to apply regression methods in HSI and MSI

The development of a multivariate regression model is not a trivial task. Many parameters must be optimized before assessing the final validity of the model [21]. This is especially relevant with HSI and MSI, since we often trend to believe that a regression model made from bulk concentrations is valid for all the pixels in the image. This is partially true. Nevertheless, certain precautions must be considered beforehand.

One of the key steps to perform a reliable regression model is the construction of the **X** matrix for the calibration step. **X** must contain all the relevant spectral information linked to the property object to be quantified, together with a sound concentration range (**y**). There are several relevant strategies to create **X** (Fig. 1):

- Extraction of the mean spectrum of a region of interest from an image where we can quantify the parameter to be measured.

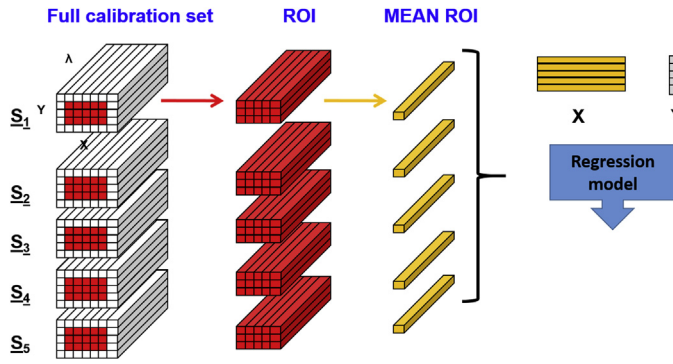

FIGURE 1 Development of the **X** matrix from different hyperspectral imaging or multispectral imaging samples by extracting the region of interest (RoI).

- Calculating the mean spectrum of a whole image where we can quantify the parameter to be measured.
- Prepare artificial samples in the laboratory containing all the compounds and measure the mean spectrum for each sample. This is especially relevant in pharmaceutical production, where it is easy to know the final concentration of the compounds [22].

The way this calibration set is constructed is essential when the final prediction is made on an HSI or MSI image, since all pixels should, in theory, be within the calibration range of **y**. Therefore, several points must be considered beforehand.

3.1 Bulk concentration versus pixel concentration

Normally the **X** matrix is constructed considering the calibration range of the bulk concentration of one compound. For example, if we expect to find 10 ppm of any compound in a sample, the regression model is constructed in such a way that we collect samples that span as much as possible between the 10 ppm. This, in natural samples is very complex, since the natural variability of the sample plays a fundamental role. Then, the regression model is constructed and validated with as many samples as possible. And this is another problem, since it is necessary to obtain the reference values of those samples need. The big problem arises when pixel-wise prediction in a new sample is performed. The regression model is constructed with bulk concentrations using mean spectra, while the prediction is normally made pixel by pixel. The problem is that the pixels of the new sample might not contain the compound that we are quantifying or, moreover, that the pixels can contain a concentration of that compound much higher than the maximum concentration of the calibration range. In this sense, Zhang et al. [23] showed this fact in the quantitation of different chlorophyll pigments in spinach (Fig. 2). Here it can

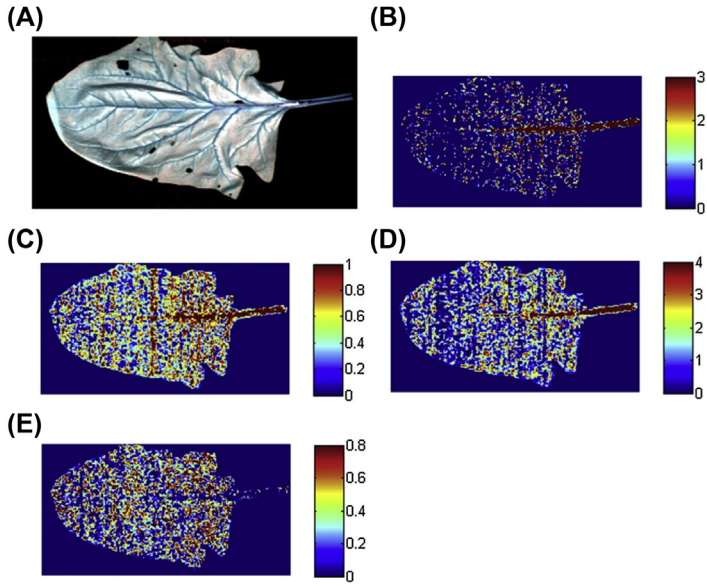

FIGURE 2 Raw image (A), prediction maps of chlorophyll-a (B), chlorophyll-b (C), total chlorophyll (D), and carotenoids (E) by applying the corresponding partial least square models using optimal wavelengths on a randomly selected image. *Figure extracted from C. Zhang, Q. Wang, F. Liu, Y. He, Y. Xiao, Rapid and non-destructive measurement of spinach pigments content during storage using hyperspectral imaging with chemometrics, Measurement 97 (2017) 149–155. https://doi.org/10.1016/j.measurement.2016.10.058. with the permission of Elsevier.*

be seen how the concentration of the chlorophyll pigments in many of the pixels belonging to the spinach are out of the available calibration range.

This is especially relevant in natural products, where the calibration matrices are normally built with the mean spectra of the whole product. Moreover, not all the spectra extracted from the image contain features that comply with the concentration range selected or even with the compound to be quantified. This issue is difficult to solve, since many times the reference methods require a huge volume of samples and this is normally done by taking an amount of samples to calculate one single reference value.

3.2 Model optimization. Validation, validation, and more validation

Many parameters can be used to validate a regression model, like, for instance, the root mean square error (RMSE) and the standard error (SE), regression coefficients or bias, among others in calibration, as well as in internal and external validation. Nevertheless, one of the key aspects that must be fulfilled, no matter which parameter to be used, is the development of intensive validation [24].

As pointed out by Westad and Marini [24], validation is one of the most important aspects in science. When it comes to validate a regression model, validation refers to the ability of the model to predict the amount that has been previously obtained in external samples by the reference method (i.e., samples whose amount is known but were not used in the construction of the calibration model). In this sense, we can count with what is known as external validation sets and cross-validation (CV) sets.

External validation sets are normally generated by splitting the bulk amount of calibration samples into two subgroups (training and test sets) [25]. This can be done by using different algorithms that span the variability of **X** and the calibration range of **y** in both training and test sets. This approach is subjected to the inner structure of the data, and it only works fine when there are not uncontrolled variation sources in the data. CV performed at any level [24] gives important information about the stability of the model and the plausible sources of variation and outlier samples. And as Westad and Marini proposed [24], CV must be performed in the test set even if a test set has been defined.

Validating a regression model in HSI and MSI is not an easy task due to the issues reported before. Normally all models are constructed from the bulk concentration of the compound that wants to be quantified. This might lead underestimations in a validation step that is normally performed by using the mean spectra. In any case, validation is a complex step that can be done in multiple ways and sometimes a good choice is to combine different validation methodologies to assess the validity of the model (without falling into the temptation of choosing the methodology that gives the best result, but considering the deviations between the different methodologies applied).

3.3 Steps to make a good regression model

It is extremely difficult to establish a flowchart of the different steps to make a good regression model; it is more difficult to define what a "good" regression model means. In general, we can affirm that a good regression model is not the one that better calibrates, but the one that better predicts. Although it seems an obvious statement, the underlying truth is that sometimes we are driven by the figures of merit of the calibration set, without paying much attention to the figures of merit of the validation set and the comparison between calibration (training) and validation (test).

Arguing that the following steps might change in each specific case, when we develop a regression model these are some steps that can always be followed considering that the simpler the model is, the better, more reliable and robust will be:

1) Reference values: Consider that the reference values are well calculated and that the uncertainty in the sampling and calculation is also well known.

That uncertainty can mark the development of further regression models, since the error of the multivariate method must be in accordance with the standard error of laboratory.

2) As many samples as possible, or not: When dealing with natural products, the most important fact to consider is to span all spectral covariability toward the property to be quantified. That is, HSI and MSI are extremely difficult, since most of the calibration models are calculated from mean spectra of the samples. Therefore, having a huge amount of samples does not guarantee that the whole calibration range is covered. If the available set of samples is reduced, at least it must be as much representative as possible of the features of the population.

3) Choose an HSI and MSI system and a regression method: Normally, we use the HSI and MSI devices that we have in our laboratories. Moreover, they normally measure in the NIR and visible spectral ranges. It might happen that the signal of the compound that we want to quantify is not very intense in that spectral range or that is overlapped with matrix effects or, simply it does not absorb in that spectral range. Moreover, when choosing regression method, bear in mind that most of natural systems have a linear dependency with absorbance. Therefore, linear models could be advisable. Sometimes, it is a question of preprocessing and variable selection to make them work properly.

4) Choose a validation method: There are many alternatives in the literature from splitting the calibration samples into two sets until CV. The method chosen should be that one that better suits with the type of data and nature of the sample. Moreover, bear in mind that even if an external test set is used, CV of the calibration (training) set should be applied as well [24].

5) Preprocessing: There are many preprocessing methodologies proposed in the literature. The preprocessing to be applied will depend on the type of spectral signature and the matrix effects that the samples can have [15,16,26].

6) Variable selection: Sometimes, we trend to use all the variables that we measure with the cameras. Nevertheless, there are many variables that do not contain information or that can have uncorrelated information. Multivariate models deal with those variables until certain degree. Nevertheless, in order to make the model more parsimonious, elimination of those variables is sometimes needed.

7) Figures of merit: One important step is the optimization of parameters such as the number of latent variables in linear models, tolerance levels in SVR,

or the architecture of a net in ANN. All these parameters need to be optimized by using figures of merit like RMSE, bias, SE, among others. Nevertheless, the optimization must be always done comparing the results in the training, CV, and test sets. This way, fluctuations in the models, plausible outliers, inconsistent data groups, or hints about different preprocessing methods or different variable grouping can be detected and, thus, the model can be optimized.

8) Repeat and check: this is the key point. Repeat steps 3 to 7 until the results are optimal; or, at least, as good as possible. There is neither handbook nor manuscript that can assess the absolute conditions for a regression model to work in all the cases. Each regression model needs to be optimized considering all the previous aspects. A comparison between the different alternatives of the model must be done (see, for instance, Table 4 in Ref. [22]).

4. Applications

4.1 Food

In general, regression methods are widely applied when visible and NIR HSI is used, becoming a powerful tool for the nondestructive prediction of quality parameters, especially in agricultural and food products, being an alternative to the traditional and destructive methods [4]. Nevertheless, most of these studies have been carried out in static conditions, being the main challenge the development of real-time and online applications, in which chemometric takes a great importance [27].

Regarding agricultural products, most research studies have been carried out on fruits for predicting quality parameters of interest for the consumer, such as soluble solids content, firmness, or the IQI (internal quality index) [28,29] (Fig. 3). According to Table 1, while there are many works related to the prediction of sugar, moisture content, and firmness, just few works used HSI for the prediction of minor components.

Prediction of minor components is not common in fruits and vegetables due to the fact that the water band dominates the spectrum in the NIR region, and it makes difficult the measurement of these minor constituents [64]. In contrast, one of these works carried out by Baiano et al. [38] obtained good correlation for pH and titratable acidity in grapes despite the low concentration of these. It must be said that authors have a broad range for both parameters since white and red/black grapes were analyzed, essential for the development of robust and accurate models.

Meat and fish industry have a great importance around the world, so that several works have been already done to analyze the feasibility of VIS-NIR HSI to establish adequate quality parameters (Table 2). Freshness and

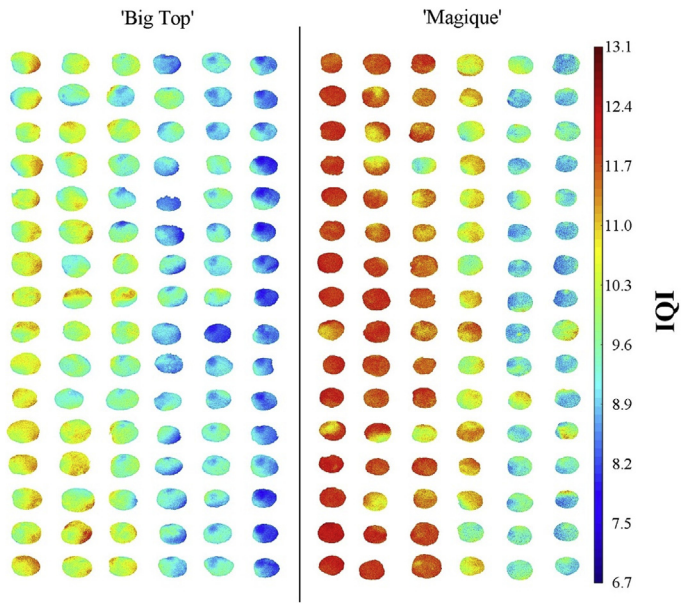

FIGURE 3 Visualization of internal quality index (IQI) prediction using partial least squares and optimal wavelengths for different cultivars of nectarines. *Extracted from S. Munera, J.M. Amigo, J. Blasco, S. Cubero, P. Talens, N. Aleixos, Ripeness monitoring of two cultivars of nectarine using VIS-NIR hyperspectral reflectance imaging, Journal of Food Engineering 214 (2017) 29–39. https://doi.org/10.1016/j.jfoodeng.2017.06.031. Reproduced with permission of Elsevier.*

tenderness (Fig. 4) are the most important quality attributes for consumers, and it is highly correlated with product sales [88]; thus, the main objective of most research works has been the prediction of quality or freshness attributes and the presence of microbial in meat [66,89].

Recently, Yang et al. [66] measured the TVC in spiced beef during the storage in the wavelength range 400−1000 nm combined with wavelet transform and multiway PLS (N-PLS). Furthermore, other parameters have been measured to determine the meat quality and freshness, like the moisture content, color, pH, and the protein content, as well as sensory attributes [3,69,73,90].

Likewise, in the case of fish products, as quality deterioration occurs rapid during the life of the product, the evaluation of chemical spoilage and freshness is essential. Infact fish was measured using VIS-NIR imaging in different applications in order to determine parameters related to its quality. A parameter used as index of the chemical spoilage is the K value based on the nucleotide degradation, has been predicted in grass carp and fish fillets by Cheng et al. [72]. To develop the models, they applied LS-SVM and MLR together with different variable selection methods.

TABLE 1 Overview of near-infrared hyperspectral imaging in agricultural products.

Product	Parameters	Regression method	Spectral range (nm)	References
Apple	Hardness, firmness, SSC firmness, SSC	PLS MLR, PLS	600–1000 500–1000	[30] [31] [32]
Banana	Moisture, firmness, SSC	MLR, PLS	400–1000	[33]
Blueberries	Firmness, SSC	PLS		[34,35]
Broccoli	Glucosinolate	PLS	450–900, 950–1650	[36]
Corn	Oil, moisture	MLR, PLS		[37]
Grape	Acidity, SSC	PLS	400–1000	[38]
Grape seed	Flavonols	PLS		[39]
Maize	Fungal development Moisture	PLS PLS	1000–2498 400–1000	[40] [41]
Mango	Moisture distribution	MLR, PLS	400–1000	[42]
Nectarines	Firmness, IQI (internal quality index)	PLS	600–950	[28,29]
Melon	Hardness, SSC	PLS	900–1700	[43]
Rocket leaves	Ripeness	PLS	400–800	[44]
Mushrooms	Moisture, color, texture Moisture	PCR, MLR PLS	400–1000	[45] [46]
Pepper plants	Total nitrogen	PLS	380–1030	[47]
Rice plants	Nitrogen	PLS	400–1000	[48]
Seed rape	Seed yield Soluble protein content	PLS PLS	380–1030	[49] [50]
Soybean	Color Drought stress	PLS PLS	400–1000 420–780	[51] [52]
Spinach leaves	Pigment content	PLS	874–1734	[23]
Tea leaves	Color compounds	PLS	380–1030	[53]

Continued

TABLE 1 Overview of near-infrared hyperspectral imaging in agricultural products.—cont'd

Product	Parameters	Regression method	Spectral range (nm)	References
Apple	Waxed detection	SVM, BP-ANN	550–1710	[54]
Banana	Moisture, hardness, fracturability	PLS, SVM	950–1650	[55]
Cabbage	Nitrogen	PLS, SMLR, ANN	410–1090	[56]
Grapes	Anthocyanin Pesticides	PLS, SVR, ANN PLS, SVR, ANN	400–1000/ 900–1700 350–1052	[57] [58]
Peaches	Cold injury	ANN	900–1700	[59]
Pear	Sugar	PLS, LS-SVM, BP-ANN	400–1000	[60]
Pistachio kernels	Moisture, texture	PLS, ANN	400–1000	[61]
Rubber trees	Foliar phosphorus	PLS, MLR, ANN	350–2500	[62]
Tea leaves	Color components	LS-SVM	380–1030	[53]
Wheat	Fusarium resistance	SVM	400–1000/ 1000–2500	[63]

ANN, Artificial neural networks; *BP-ANN*, Back propagation artificial neural networks; *LS-SVM*, Least squares-support vectors machine; *MLR*, Multiple linear regression; *PLS*, Partial least squares; *SMLR*, Step-wise multi-linear regression; *SSC*, Soluble solid content; *SVM*, Support vector machine.

The maintenance of quality and safety of food is a legal requirement and, since fresh products are the most sensitive to be affected, most research works are dedicated to investigating them. However, there are also studies related to other types of products, not as perishable as fresh food, but also with high standards of quality (Table 3). The presence of contaminants in food products, like melamine in powder milk or the purity of organic flour, has been deeply studied by different authors [93,97]. Likewise, HSI and linear regression methods have been also used to assess different processes through the control of specific parameters, like the total acid content and the moisture content during the fermentation of the vinegar [95] or the acidity and viscosity in the frying oils [92].

TABLE 2 Overview of near-infrared hyperspectral imaging in other food products (fish and meat).

Product	Parameters	Regression	Spectral range (nm)	References
Beef Beef (dried)	Chemical composition Total visible count (TVC) Water content	PLS PLS MLR	325–1100	[65] [66] [67]
Beef	Tenderness	PLS	1000–2500	[68]
Chicken Chicken breast fillet	Moisture content Thibarbituric acid–reactive substances (TBARS), TVC, pseudomonas loads	PLS PLS PLS	897–1752	[69] [27] [70]
Crabs	Edible meat content	PLS		[71]
Fish	K	PLS		[72]
Ham	Water content, protein	PLS		[73]
Lamb	Chemical composition	PLS	900–1700	[74]
Pork Cured pork slices	Freshness Biogenic amine index (BAI) Total volatile basic nitrogen (TVB-N)	PLS MLR MLR		[75] [76] [66]
Prawns	Moisture content	MLR, PLS	380–1100	[77]
Salmon	Freshness	PLS	400–1000, 897–1753	[67]
Seafood	Core temperature	PLS	900–2500	[78]
Turkey	Moisture, color, pH	PLS		[3]

Continued

TABLE 2 Overview of near-infrared hyperspectral imaging in other food products (fish and meat).—cont'd

Product	Parameters	Regression	Spectral range (nm)	References
Beef	Adulteration Moisture content, color Moisture content, storage time	LS-SVM MLR, SVM PLS, BP-ANN	496–1000 400–1000 320–1100	[79] [80] [81]
Chicken	Springiness	PLS, ANN	400–1000	[82]
Grass carp	K TVB-N	LS-SVM PLS, LS-SVM	308–1105 308–1105	[72] [83]
Pork	TVB-N pH	BP-ANN SVR	1280, 1440, 1660 400–800	[84] [85]
Prawns	Moisture content	LS-SVM	380–1100	[77]
Salmon	Freshness	LS-SVM	400–1000/897–1753	[67]
Smoked salmon	TVB-N	SVM	400–1000	[86]
Tilapia	TVB-N, TAC	RBF-ANN	325–1098	[87]

ANN, Artificial neural networks; *MLR*, Multiple linear regression; *PLS*, Partial least squares; *SVM*, Support vector machine; *SVR*, Support vector regression.

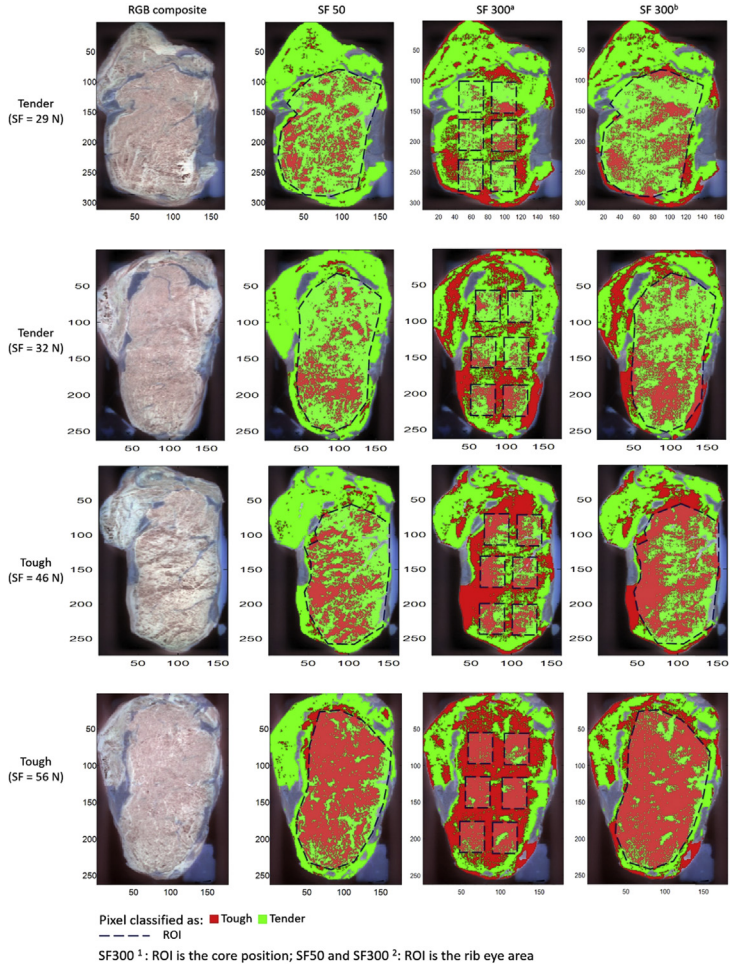

FIGURE 4 Tenderness distribution maps for beef longissimus muscle from PLS-DA models using the mean spectrum of the whole rib eye area. SF50 and SF300b: the region of interest (RoI) is the rib eye area. SF300a: the RoI is the core position.

4.2 Pharmaceutical production

The application of HSI and MSI in pharmaceutical production and drugs development will be thoughtfully treated in another book chapter. Nevertheless, we consider that it is important to remark some aspects to what concerns the application of regression models in these types of samples. Since the implementation of the quality by design and the process analytical technologies [5], HSI and MSI together with NIR have experienced a high increase not only in the pharmaceutical production but also in new drugs development [104–108].

TABLE 3 Overview of near-infrared hyperspectral imaging in other products.

Product	Parameters	Regression	Spectral range (nm)	References
Egg	α-Linolenic, eicosapentaenoic, docosahexaenoic	PLS	900–1700	[91]
Frying oils	Acid value, total polar component, viscosity	PLS	400–1750	[92]
Milk powder	Melamine	PLS	990–1700	[93]
Spelt flour	Purity	PLS	900–1700	[94]
Vinegar	Total acid content, moisture	PLS	400–1000	[95]
Wheat Wheat flour	Leaf nitrogen concentration Adulteration Bulk density	PLS PCR PLS	400–1000 897–1753 400–1000	[96] [97] [98]
Cheese	Hardness	PLS, ANN	400–1000	[99]
Honey	Adulteration	SVM, ANN	400–1000	[100]
Seawater	Detection microplastics	SVM	900–1700	[101]
Soil	Organic carbon Characteristics	PLS, MLR, SVM SVM, BP-ANN	350–2500 350–3500	[102] [103]

ANN, Artificial neural networks; *PCR,* Principal component regression; *PLS,* Partial least squares; *SVM,* Support vector machine.

In the case of solid dosage forms [22,104], developing regression models is much easier than in natural products. Due to strict regulations, the composition of solid dosage forms must be perfectly known. Moreover, the amount of compounds forming the solid dosage form is normally limited to a small number. Another advantage when using HSI-NIR is the no presence (or very little presence) of water, allowing the NIR spectra obtained to reflect features of all the compounds in the tablet. These benefits, together with the need of nondestructive methods of analysis have encouraged many pharmaceutical companies to adopt and adapt HSI and HSI methodologies in their production area. As for example, Khorasani et al. developed a methodology [107,109,110]

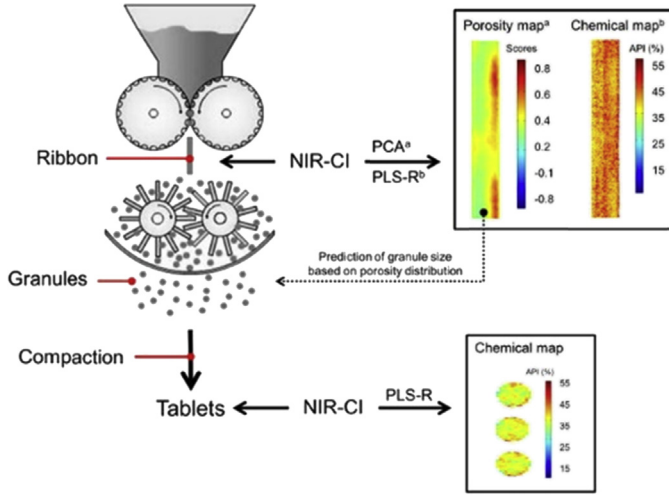

FIGURE 5 An overview of the overall process monitoring of roll compaction and tableting; the implementation of NIR-CI to gain information related to the physical or chemical properties of intermediate or final product. *Extracted from M. Khorasani, J.M. Amigo, C.C. Sun, P. Bertelsen, J. Rantanen, Near-infrared chemical imaging (NIR-CI) as a process monitoring solution for a production line of roll compaction and tableting, European Journal of Pharmaceutics and Biopharmaceutics 93 (2015). https://doi.org/10.1016/j.ejpb.2015.04.008. Reproduced with permission of Elsevier.*

that was able to control the quality not only of the final tablets but also in the granulation and blending steps (Fig. 5).

In this case, regression models were developed using tablets prepared in the laboratory with perfectly known concentration of all ingredients for both the ribbons and the final tablets (Fig. 6) and using PLS-R on NIR HSI images.

The main issue in pharmaceutical production using HSI and MSI is the technological challenge of being able to measure the whole volume of samples produced per minute. Further development in instrumentation technology, speed, and data processing is needed to fully employ chemical imaging in the manufacturing process.

5. Conclusions

During this chapter, we have revised some of the most prominent applications of regression models in HSI and MSI with especial emphasis in food research and a hint in what concerns pharmaceutical production. The first part of the chapter was focused on a brief theoretical background to understand the essential concepts of multivariate regression models. We mainly focused on linear regression models, acknowledging that multivariate regression models of higher complexity could also be used.

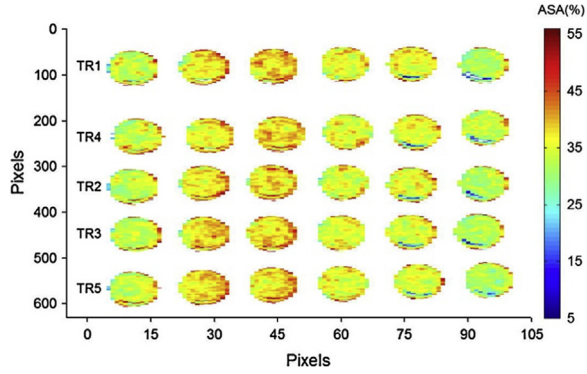

FIGURE 6 Active principal ingredient (API) distribution map of tablets predicted by partial least squares regression (PLS-R) model. *Extracted from M. Khorasani, J.M. Amigo, C.C. Sun, P. Bertelsen, J. Rantanen, Near-infrared chemical imaging (NIR-CI) as a process monitoring solution for a production line of roll compaction and tableting, European Journal of Pharmaceutics and Biopharmaceutics 93 (2015). https://doi.org/10.1016/j.ejpb.2015.04.008. Reproduced with permission of Elsevier.*

To our understanding, the most important part of this book chapter is Section 3. There, we set the main steps to be done when applying any kind of regression method (and, to some extent, classification models even though they are out of the scope of this chapter). One of the key aspects that we wanted to highlight is the difference between constructing a model using mean spectra coming from bulk samples and the pixel-wise prediction that we adopted in HSI and MSI. For sure, this is a key point in which we need to continue working in order to make models that are more reliable and to be able to predict within the calibration range.

Concerning applications, the most conflictive area is the application of regression models in food research. Food samples are by nature a complex mixture of many major and minor compounds, and, sometimes, reliable regression models for those minor compounds are difficult to develop due to the complexity of the sample or the nature of the minor compounds. One of the major problems here is to avoid or model the interference of water, since this is one of the major compounds in food samples and, at the same time, a compound with high reflectance bands in the NIR spectral region. In pharmaceutical production, the main limitations come from the instrumentation, being strongly needed faster and reliable HSI and MSI systems to comply with the requirements of an industry that is able to manufacture thousands of tablets per minute.

References

[1] J.M. Amigo, H. Babamoradi, S. Elcoroaristizabal, Hyperspectral image analysis. A tutorial, Analytica Chimica Acta 896 (2015) 34–51, https://doi.org/10.1016/j.aca.2015.09.030.

[2] Y.Z. Feng, G. Elmasry, D.W. Sun, A.G.M. Scannell, D. Walsh, N. Morcy, Near-infrared hyperspectral imaging and partial least squares regression for rapid and reagentless determination of Enterobacteriaceae on chicken fillets, Food Chemistry 138 (2013) 1829–1836, https://doi.org/10.1016/j.foodchem.2012.11.040.

[3] A. Iqbal, D.W. Sun, P. Allen, Prediction of moisture, color and pH in cooked, pre-sliced Turkey hams by NIR hyperspectral imaging system, Journal of Food Engineering 117 (2013) 42–51, https://doi.org/10.1016/j.jfoodeng.2013.02.001.

[4] J.M. Amigo, I. Martí, A. Gowen, Hyperspectral imaging and chemometrics. A perfect combination for the analysis of food structure, composition and quality, Data Handling in Science and Technology 28 (2013) 343–370, https://doi.org/10.1016/B978-0-444-59528-7.00009-0.

[5] A.A. Gowen, J.M. Amigo, Applications of Spectroscopy and Chemical Imaging in Pharmaceutics, in: Handbook of Biophotonics, 2012, https://doi.org/10.1002/9783527643981.bphot083.

[6] P. Geladi, J. Burger, T. Lestander, Hyperspectral imaging: calibration problems and solutions, Chemometrics and Intelligent Laboratory System 72 (2004) 209–217, isi:000222986900012.

[7] J. Burger, P. Geladi, Hyperspectral NIR image regression part I: calibration and correction, Journal of Chemometrics 19 (2005) 355–363, https://doi.org/10.1002/cem.986.

[8] J. Burger, P. Geladi, Hyperspectral NIR image regression part II: dataset preprocessing diagnostics, Journal of Chemometrics 20 (2006) 106–119, https://doi.org/10.1002/cem.986.

[9] T.T. Lied, P. Geladi, K.H. Esbensen, Multivariate image regression (MIR): implementation of image PLSR - first forays, Journal of Chemometrics 14 (2000) 585–598, https://doi.org/10.1002/1099-128X(200009/12)14:5/6<585::AID-CEM627>3.0.CO;2-Q.

[10] T. Næs, T. Isaksson, T. Fearn, Davies, A user-friendly guide to multivariate calibration and classification, Technometrics 46 (2004) 108–110. https://doi.org/10.1198/004017004000000167.

[11] S. Puntanen, Methods of multivariate analysis, third edition, in: International Statistical Review, 81, 2013, pp. 328–329. https://doi.org/10.1111/insr.12020_20.

[12] I.T. Jolliffee, A note on the use of principal components in regression, Journal of the Royal Statistical Society: Series A C. 31 (1982) 300–303.

[13] S. Wold, M. Sjöström, L. Eriksson, PLS-regression: a basic tool of chemometrics, Chemometrics and Intelligent Laboratory Systems (2001) 109–130. https://doi.org/10.1016/S0169-7439(01)00155-1.

[14] M. Andersson, A comparison of nine PLS1 algorithms, Journal of Chemometrics 23 (2009) 518–529. https://doi.org/10.1002/cem.1248.

[15] Å. Rinnan, F. van den Berg, S.B. Engelsen, A. Rinnan, F. van den Berg, S.B. Engelsen, Review of the most common pre-processing techniques for near-infrared spectra, Trends in Analytical Chemistry (Reference Ed.) 28 (2009) 1201–1222. https://doi.org/10.1016/j.trac.2009.07.007.

[16] M. Vidal, J.M. Amigo, Pre-processing of hyperspectral images. Essential steps before image analysis, Chemometrics and Intelligent Laboratory Systems 117 (2012) 138–148. https://doi.org/10.1016/j.chemolab.2012.05.009.

[17] C. Cortes, V. Vapnik, Support-vector networks, Machine Learning 20 (1995) 273–297. https://doi.org/10.1023/A:1022627411411.

[18] H. Drucker, C.J.C. Burges, L. Kaufman, A. Smola, V. Vapnik, Support vector regression machines, in: Adv. Neural Inf. Process. Syst. 9 Proc. 1996 Conf., 1997, pp. 155–161. http://books.google.com/books?hl=en&lr=&id=QpD7n95ozWUC&pgis=1.

[19] E. Boser, N. Vapnik, I.M. Guyon, T.B. Laboratories, A training algorithm margin for optimal classifiers, in: 5th Annu. Work. Comput. Learn. Theory., vol. 8, 1992, pp. 144−152.

[20] F. Marini, R. Bucci, A.L. Magrì, A.D. Magrì, Artificial neural networks in chemometrics: history, examples and perspectives, Microchemical Journal (2008). https://doi.org/10.1016/j.microc.2007.11.008.

[21] J. Burger, P. Geladi, Hyperspectral NIR imaging for calibration and prediction: a comparison between image and spectrometer data for studying organic and biological samples, Analyst 131 (2006) 1152−1160, isi:000244355200013.

[22] C. Ravn, E. Skibsted, R. Bro, Near-infrared chemical imaging (NIR-CI) on pharmaceutical solid dosage forms-comparing common calibration approaches, Journal of Pharmaceutical and Biomedical Analysis 48 (2008) 554−561. https://doi.org/10.1016/j.jpba.2008.07.019.

[23] C. Zhang, Q. Wang, F. Liu, Y. He, Y. Xiao, Rapid and non-destructive measurement of spinach pigments content during storage using hyperspectral imaging with chemometrics, Measurement 97 (2017) 149−155. https://doi.org/10.1016/j.measurement.2016.10.058.

[24] F. Westad, F. Marini, Validation of chemometric models - a tutorial, Analytica Chimica Acta 893 (2015) 14−24. https://doi.org/10.1016/j.aca.2015.06.056.

[25] Q.S. Xu, Y.Z. Liang, Y.P. Du, Monte Carlo cross-validation for selecting a model and estimating the prediction error in multivariate calibration, Journal of Chemometrics (2004). https://doi.org/10.1002/cem.858.

[26] J. Burger, P. Geladi, Spectral pre-treatments of hyperspectral near infrared images: analysis of diffuse reflectance scattering, Journal of Near Infrared Spectroscopy 15 (2007) 29−37. https://doi.org/10.1255/jnirs.717.

[27] Z. Xiong, D.W. Sun, H. Pu, A. Xie, Z. Han, M. Luo, Non-destructive prediction of thiobarbituric acid reactive substances (TBARS) value for freshness evaluation of chicken meat using hyperspectral imaging, Food Chemistry 179 (2015) 175−181. https://doi.org/10.1016/j.foodchem.2015.01.116.

[28] S. Munera, J. Blasco, J.M. Amigo, S. Cubero, P. Talens, N. Aleixos, Use of hyperspectral transmittance imaging to evaluate the internal quality of nectarines, Biosystems Engineering 182 (2019) 54−64.

[29] S. Munera, J.M. Amigo, J. Blasco, S. Cubero, P. Talens, N. Aleixos, Ripeness monitoring of two cultivars of nectarine using VIS-NIR hyperspectral reflectance imaging, Journal of Food Engineering 214 (2017) 29−39. https://doi.org/10.1016/j.jfoodeng.2017.06.031.

[30] M. Huang, R. Lu, Postharvest biology and technology apple mealiness detection using hyperspectral scattering technique, Postharvest Biology and Technology 58 (2010) 168−175. https://doi.org/10.1016/j.postharvbio.2010.08.002.

[31] J. Qin, R. Lu, Y. Peng, Prediction of Apple Internal Quality Using Spectral Absorption and Scattering Properties, vol. 52, 2009, pp. 499−507.

[32] F. Mendoza, R. Lu, D. Ariana, H. Cen, B. Bailey, Integrated spectral and image analysis of hyperspectral scattering data for prediction of apple fruit firmness and soluble solids content, Postharvest Biology and Technology 62 (2011) 149−160. https://doi.org/10.1016/j.postharvbio.2011.05.009.

[33] P. Rajkumar, N. Wang, G. EImasry, G.S.V. Raghavan, Y. Gariepy, Studies on banana fruit quality and maturity stages using hyperspectral imaging, Journal of Food Engineering 108 (2012) 194−200. https://doi.org/10.1016/j.jfoodeng.2011.05.002.

[34] G.A. Leiva-valenzuela, R. Lu, J. Miguel, Prediction of firmness and soluble solids content of blueberries using hyperspectral reflectance imaging, Journal of Food Engineering 115 (2013) 91−98. https://doi.org/10.1016/j.jfoodeng.2012.10.001.

[35] G.A. Leiva-valenzuela, R. Lu, J. Miguel, Assessment of internal quality of blueberries using hyperspectral transmittance and reflectance images with whole spectra or selected wavelengths, Innovative Food Science & Emerging Technologies (2014). https://doi.org/10.1016/j.ifset.2014.02.006.

[36] J.M. Hernández-Hierro, C. Esquerre, J. Valverde, S. Villacreces, K. Reilly, M. Gaffney, M.L. González-Miret, F.J. Heredia, C.P. O'Donnell, G. Downey, Preliminary study on the use of near infrared hyperspectral imaging for quantitation and localisation of total glucosinolates in freeze-dried broccoli, Journal of Food Engineering 126 (2014) 107−112. https://doi.org/10.1016/j.jfoodeng.2013.11.005.

[37] R.P. Cogdill, G.R. Rippke, S.J. Bajic, R.W. Jones, Single-Kernel Maize Analysis by Near-Infrared Hyperspectral Imaging Single-Kernel Maize Analysis by Near-Infrared Hyperspectral Imaging, 2004.

[38] A. Baiano, C. Terracone, G. Peri, R. Romaniello, Application of hyperspectral imaging for prediction of physico-chemical and sensory characteristics of table grapes, Computers and Electronics in Agriculture 87 (2012) 142−151. https://doi.org/10.1016/j.compag.2012.06.002.

[39] F.J. Rodríguez-pulido, J.M. Hernández-hierro, J. Nogales-bueno, B. Gordillo, M.L. González-miret, F.J. Heredia, A novel method for evaluating flavanols in grape seeds by near infrared hyperspectral imaging, Talanta 122 (2014) 145−150. https://doi.org/10.1016/j.talanta.2014.01.044.

[40] P.J. Williams, P. Geladi, T.J. Britz, M. Manley, Investigation of fungal development in maize kernels using NIR hyperspectral imaging and multivariate data analysis, Journal of Cereal Science 55 (2012) 272−278. https://doi.org/10.1016/j.jcs.2011.12.003.

[41] M. Huang, W. Zhao, Q. Wang, M. Zhang, Q. Zhu, Prediction of moisture content uniformity using hyperspectral imaging technology during the drying of maize kernel, International Agrophysics 29 (2015) 39−46. https://doi.org/10.1515/intag-2015-0012.

[42] Y.Y. Pu, D.W. Sun, Vis-NIR hyperspectral imaging in visualizing moisture distribution of mango slices during microwave-vacuum drying, Food Chemistry 188 (2015) 271−278. https://doi.org/10.1016/j.foodchem.2015.04.120.

[43] Y. Liu, H. Pu, D.W. Sun, Hyperspectral imaging technique for evaluating food quality and safety during various processes: a review of recent applications, Trends in Food Science & Technology 69 (2017) 25−35. https://doi.org/10.1016/j.tifs.2017.08.013.

[44] M.M.A. Chaudhry, M.L. Amodio, F. Babellahi, M.L.V. de Chiara, J.M. Amigo Rubio, G. Colelli, Hyperspectral imaging and multivariate accelerated shelf life testing (MASLT) approach for determining shelf life of rocket leaves, Journal of Food Engineering 238 (2018) 122−133. https://doi.org/10.1016/j.jfoodeng.2018.06.017.

[45] A.A. Gowen, C.P. O'Donnell, M. Taghizadeh, P.J. Cullen, J.M. Frias, G. Downey, Hyperspectral imaging combined with principal component analysis for bruise damage detection on white mushrooms (*Agaricus bisporus*), Journal of Chemometrics 22 (2008) 259−267, isi:000255294600012.

[46] M. Taghizadeh, A. Gowen, C.P. O'Donnell, Prediction of white button mushroom (*Agaricus bisporus*) moisture content using hyperspectral imaging, Sensing and Instrumentation for Food Quality and Safety 3 (2009) 219−226. https://doi.org/10.1007/s11694-009-9088-y.

[47] K.Q. Yu, Y.R. Zhao, X.L. Li, Y.N. Shao, F. Liu, Y. He, Hyperspectral imaging for mapping of total nitrogen spatial distribution in pepper plant, PLoS One 9 (2014) 1−19. https://doi.org/10.1371/journal.pone.0116205.

[48] H. Onoyama, C. Ryu, M. Suguri, M. Iida, Potential of hyperspectral imaging for constructing a year-invariant model to estimate the nitrogen content of rice plants at the panicle initiation stage, IFAC Proceedings Volumes (2013). https://doi.org/10.3182/20130828-2-SF-3019.00054.

[49] X. Zhang, Y. He, Rapid estimation of seed yield using hyperspectral images of oilseed rape leaves, Industrial Crops and Products 42 (2013) 416–420. https://doi.org/10.1016/j.indcrop.2012.06.021.

[50] C. Zhang, F. Liu, W. Kong, Y. He, Application of visible and near-infrared hyperspectral imaging to determine soluble protein content in oilseed rape leaves, Sensors (Switzerland) 15 (2015) 16576–16588. https://doi.org/10.3390/s150716576.

[51] M. Huang, Q. Wang, M. Zhang, Q. Zhu, Prediction of color and moisture content for vegetable soybean during drying using hyperspectral imaging technology, Journal of Food Engineering 128 (2014) 24–30. https://doi.org/10.1016/j.jfoodeng.2013.12.008.

[52] C. Mo, M.S. Kim, G. Kim, E.J. Cheong, J. Yang, J. Lim, Detecting drought stress in soybean plants using hyperspectral fluorescence imaging, Journal of Biosystems Engineering 40 (2016) 335–344. https://doi.org/10.5307/jbe.2015.40.4.335.

[53] C. Xie, X. Li, Y. Shao, Y. He, Color measurement of tea leaves at different drying periods using hyperspectral imaging technique, PLoS One 9 (2014) 1–15. https://doi.org/10.1371/journal.pone.0113422.

[54] H. Wang, H. Zhu, Z. Zhao, The study on increasing the identification accuracy of waxed apples by hyperspectral imaging technology, Multimedia Tools and Applications (2018).

[55] Y. Pu, M. Zhao, C.O. Donnell, D. Sun, Nondestructive quality evaluation of banana slices during microwave vacuum drying using spectral and imaging techniques, Drying Technology (2018) 3937. https://doi.org/10.1080/07373937.2017.1415929.

[56] C. Suming, C.Y. Wang, C.Y. Tsai, Evaluation of nitrogen content in cabbage seedlings using hyper-spectral images, Sensing and Instrumentation for Food Quality and Safety (2008) 97–102. https://doi.org/10.1007/s11694-008-9041-5.

[57] S. Chen, F. Zhang, J. Ning, X. Liu, Z. Zhang, S. Yang, Predicting the anthocyanin content of wine grapes by NIR hyperspectral imaging, Food Chemistry 172 (2015) 788–793. https://doi.org/10.1016/j.foodchem.2014.09.119.

[58] J. Mohite, Y. Karale, S. Pappula, A. Shabeer, in: Detection of Pesticide (Cyantraniliprole) Residue on Grapes Using Hyperspectral Sensing, 10217, 2017, pp. 1–8. https://doi.org/10.1117/12.2261797.

[59] L. Pan, Q. Zhang, W. Zhang, Y. Sun, P. Hu, K. Tu, Detection of cold injury in peaches by hyperspectral reflectance imaging and artificial neural network, Food Chemistry 192 (2016) 134–141. https://doi.org/10.1016/j.foodchem.2015.06.106.

[60] D. Zhang, L. Xu, D. Liang, Fast prediction of sugar content in Dangshan pear (*Pyrus* spp .) using hyperspectral imagery data, Food Analytical Methods (2018) 2336–2345.

[61] T.M. Moghaddam, S.M.A. Razavi, M. Taghizadeh, B. Pradhan, Hyperspectral imaging as an effective tool for prediction the moisture content and textural characteristics of roasted pistachio kernels, Journal of Food Measurement and Characterization 12 (2018) 1493–1502. https://doi.org/10.1007/s11694-018-9764-x.

[62] P. Guo, Z. Shi, M. Li, W. Luo, Z. Cha, A robust method to estimate foliar phosphorus of rubber trees with hyperspectral reflectance, Industrial Crops and Products 126 (2018) 1–12. https://doi.org/10.1016/j.indcrop.2018.09.055.

[63] E. Alisaac, J. Behmann, M.T. Kuska, Hyperspectral quantification of wheat resistance to *Fusarium* head blight : comparison of two *Fusarium* species, European Journal of Plant Pathology (2018).

[64] B.M. Nicolaï, K. Beullens, E. Bobelyn, A. Peirs, W. Saeys, K.I. Theron, J. Lammertyn, Nondestructive measurement of fruit and vegetable quality by means of NIR spectroscopy: a review, Postharvest Biology and Technology 46 (2007) 99−118. https://doi.org/10.1016/j.postharvbio.2007.06.024.

[65] G. ElMasry, D.W. Sun, P. Allen, Chemical-free assessment and mapping of major constituents in beef using hyperspectral imaging, Journal of Food Engineering 117 (2013) 235−246. https://doi.org/10.1016/j.jfoodeng.2013.02.016.

[66] D. Yang, A. Lu, D. Ren, J. Wang, Detection of total viable count in spiced beef using hyperspectral imaging combined with wavelet transform and multiway partial least squares algorithm, Journal of Food Safety (2017) 1−13. https://doi.org/10.1111/jfs.12390.

[67] D. Wu, D.W. Sun, Application of visible and near infrared hyperspectral imaging for non-invasively measuring distribution of water-holding capacity in salmon flesh, Talanta 116 (2013) 266−276. https://doi.org/10.1016/j.talanta.2013.05.030.

[68] J.M. Balage, J.M. Amigo, D.S. Antonelo, M.R. Mazon, S. da Luz e Silva, Shear force analysis by core location in Longissimus steaks from Nellore cattle using hyperspectral images − a feasibility study, Meat Science 143 (2018). https://doi.org/10.1016/j.meatsci.2018.04.003.

[69] L.M. Kandpal, Hyperspectral reflectance imaging technique for visualization of moisture distribution in cooked chicken breast, Sensors (2013) 13289−13300. https://doi.org/10.3390/s131013289.

[70] Y.Z. Feng, D.W. Sun, Determination of total viable count (TVC) in chicken breast fillets by near-infrared hyperspectral imaging and spectroscopic transforms, Talanta 105 (2013) 244−249. https://doi.org/10.1016/j.talanta.2012.11.042.

[71] J.P. Wold, M. Kermit, A. Woll, Rapid nondestructive determination of edible meat content in crabs (*Cancer pagurus*) by near-infrared imaging spectroscopy, Applied Spectroscopy 64 (2010) 691−699. https://doi.org/10.1366/000370210791666273.

[72] J.H. Cheng, D.W. Sun, H. Pu, Z. Zhu, Development of hyperspectral imaging coupled with chemometric analysis to monitor K value for evaluation of chemical spoilage in fish fillets, Food Chemistry 185 (2015) 245−253. https://doi.org/10.1016/j.foodchem.2015.03.111.

[73] P. Talens, L. Mora, N. Morsy, D.F. Barbin, G. Elmasry, D. Sun, Prediction of water and protein contents and quality classification of Spanish cooked ham using NIR hyperspectral imaging, Journal of Food Engineering 117 (2013) 272−280. https://doi.org/10.1016/j.jfoodeng.2013.03.014.

[74] G. Elmasry, M. Kamruzzaman, D.W. Sun, P. Allen, Principles and applications of hyperspectral imaging in quality evaluation of agro-food products: a review, Critical Reviews in Food Science and Nutrition 52 (2012) 999−1023.

[75] X. Wang, M. Zhao, R. Ju, Q. Song, D. Hua, C. Wang, T. Chen, Visualizing quantitatively the freshness of intact fresh pork using acousto-optical tunable filter-based visible/near-infrared spectral imagery, Computers and Electronics in Agriculture 99 (2013) 41−53. https://doi.org/10.1016/j.compag.2013.08.025.

[76] W. Cheng, D.W. Sun, J.H. Cheng, Pork biogenic amine index (BAI) determination based on chemometric analysis of hyperspectral imaging data, Lebensmittel-Wissenschaft und -Technologie- Food Science and Technology 73 (2016) 13−19. https://doi.org/10.1016/j.lwt.2016.05.031.

[77] D. Wu, H. Shi, S. Wang, Y. He, Y. Bao, K. Liu, Rapid prediction of moisture content of dehydrated prawns using online hyperspectral imaging system, Analytica Chimica Acta 726 (2012) 57−66. https://doi.org/10.1016/j.aca.2012.03.038.

[78] G. Elmasry, S. Nakauchi, Noninvasive sensing of thermal treatments of Japanese seafood products using imaging spectroscopy, International Journal of Food Science and Technology 50 (2015) 1960−1971. https://doi.org/10.1111/ijfs.12863.

[79] H. Zhao, Y. Feng, W. Chen, G. Jia, Application of invasive weed optimization and least square support vector machine for prediction of beef adulteration with spoiled beef based on visible near-infrared (Vis-NIR) hyperspectral imaging, Meat Science 151 (2019) 75−81. https://doi.org/10.1016/j.meatsci.2019.01.010.

[80] Y. Liu, D. Sun, Hyperspectral imaging sensing of changes in moisture content and color of beef during microwave heating process, Food Analytical Methods (2018).

[81] D. Yang, D. He, A. Lu, D. Ren, Combination of spectral and textural information of hyperspectral imaging for the prediction of the moisture content and storage time of cooked beef, Infrared Physics & Technology (2017). https://doi.org/10.1016/j.infrared.2017.05.005.

[82] Z. Xiong, D. Sun, Q. Dai, Z. Han, X. Zeng, L. Wang, Application of visible hyperspectral imaging for prediction of springiness of fresh chicken meat, Food Analytical Methods (2014). https://doi.org/10.1007/s12161-014-9853-3.

[83] J.H. Cheng, D.W. Sun, J.H. Qu, H. Bin Pu, X.C. Zhang, Z. Song, X. Chen, H. Zhang, Developing a multispectral imaging for simultaneous prediction of freshness indicators during chemical spoilage of grass carp fish fillet, Journal of Food Engineering 182 (2016) 9−17. https://doi.org/10.1016/j.jfoodeng.2016.02.004.

[84] Q. Huang, Q. Chen, H. Li, G. Huang, Q. Ouyang, J. Zhao, Non-destructively sensing pork's freshness indicator using near infrared multispectral imaging technique, Journal of Food Engineering 154 (2015) 69−75. https://doi.org/10.1016/j.jfoodeng.2015.01.006.

[85] X. Yao, F. Cai, P. Zhu, H. Fang, J. Li, S. He, Non-invasive and rapid pH monitoring for meat quality assessment using a low-cost portable hyperspectral scanner, Meat Science 152 (2019) 73−80. https://doi.org/10.1016/j.meatsci.2019.02.017.

[86] E. Ivorra, A.J. Sánchez, S. Verdú, J.M. Barat, R. Grau, Shelf life prediction of expired vacuum-packed chilled smoked salmon based on a KNN tissue segmentation method using hyperspectral images, Journal of Food Engineering (2016). https://doi.org/10.1016/j.jfoodeng.2016.01.008.

[87] C. Shi, J. Qian, W. Zhu, H. Liu, S. Han, X. Yang, Nondestructive determination of freshness indicators for tilapia fillets stored at various temperatures by hyperspectral imaging coupled with RBF neural networks, Food Chemistry 275 (2019) 497−503. https://doi.org/10.1016/j.foodchem.2018.09.092.

[88] M. Rzepka, F. Ozogul, K. Sur, M. Michalczyk, Freshness and quality attributes of cold stored Atlantic bonito (*Sarda sarda*) gravad, Food Science and Technology (2013) 1318−1326. https://doi.org/10.1111/ijfs.12094.

[89] Y.K. Peng, J. Zhang, W. Wang, Y.Y. Li, J.H. Wu, H. Huang, X.D. Gao, W.K. Jiang, Potential prediction of the microbial spoilage of beef using spatially resolved hyperspectral scattering profiles, Journal of Food Engineering 102 (2011) 163−169, isi:000283615900008.

[90] D.F. Barbin, G. Elmasry, D.W. Sun, P. Allen, Predicting quality and sensory attributes of pork using near-infrared hyperspectral imaging, Analytica Chimica Acta 719 (2012) 30−42. https://doi.org/10.1016/j.aca.2012.01.004.

[91] N. Abdel-Nour, M. Ngadi, Detection of omega-3 fatty acid in designer eggs using hyperspectral imaging, International Journal of Food Sciences & Nutrition 62 (2011) 418−422. https://doi.org/10.3109/09637486.2010.542407.

[92] S. Kazemi, N. Wang, M. Ngadi, S.O. Prasher, Evaluation of frying oil quality using VIS/NIR hyperspectral analysis, Agricultural Engineering: International. CIGR EJournal. 18 (1999) 83–93. http://www.cigrjournal.org/index.php/Ejounral/article/view/587.

[93] J. Lim, G. Kim, C. Mo, M.S. Kim, K. Chao, J. Qin, X. Fu, I. Baek, B.K. Cho, Detection of melamine in milk powders using near-infrared hyperspectral imaging combined with regression coefficient of partial least square regression model, Talanta 151 (2016) 183–191. https://doi.org/10.1016/j.talanta.2016.01.035.

[94] W.H. Su, D.W. Sun, Facilitated wavelength selection and model development for rapid determination of the purity of organic spelt (*Triticum spelta* L.) flour using spectral imaging, Talanta 155 (2016) 347–357. https://doi.org/10.1016/j.talanta.2016.04.041.

[95] Y. Zhu, X. Zou, T. Shen, J. Shi, J. Zhao, M. Holmes, G. Li, Determination of total acid content and moisture content during solid-state fermentation processes using hyperspectral imaging, Journal of Food Engineering 174 (2016) 75–84. https://doi.org/10.1016/j.jfoodeng.2015.11.019.

[96] N. Vigneau, M. Ecarnot, G. Rabatel, P. Roumet, Potential of field hyperspectral imaging as a non destructive method to assess leaf nitrogen content in wheat, Field Crops Research 122 (2011) 25–31. https://doi.org/10.1016/j.fcr.2011.02.003.

[97] W.H. Su, D.W. Sun, Evaluation of spectral imaging for inspection of adulterants in terms of common wheat flour, cassava flour and corn flour in organic Avatar wheat (*Triticum* spp.) flour, Journal of Food Engineering 200 (2017) 59–69. https://doi.org/10.1016/j.jfoodeng.2016.12.014.

[98] Q. Zhu, Y. Xing, R. Lu, M. Huang, P.K.W. Ng, Visible/shortwave near infrared spectroscopy and hyperspectral scattering for determining bulk density and particle size of wheat flour, Journal of Near Infrared Spectroscopy 25 (2017) 116–126. https://doi.org/10.1177/0967033517704081.

[99] N. Vásquez, C. Magán, J. Oblitas, T. Chuquizuta, H. Avila-George, W. Castro, Comparison between artificial neural network and partial least squares regression models for hardness modeling during the ripening process of swiss-type cheese using spectral profiles, Journal of Food Engineering 219 (2018) 8–15. https://doi.org/10.1016/j.jfoodeng.2017.09.008.

[100] S. Shafiee, G. Polder, S. Minaei, N. Moghadam-Charkari, S. van Ruth, P.M. Kuś, Detection of honey adulteration using hyperspectral imaging, IFAC-PapersOnLine. 49 (2016) 311–314. https://doi.org/10.1016/j.ifacol.2016.10.057.

[101] J. Shan, J. Zhao, Y. Zhang, L. Liu, F. Wu, X. Wang, Simple and rapid detection of microplastics in seawater using hyperspectral imaging technology, Analytica Chimica Acta 1050 (2019) 161–168. https://doi.org/10.1016/j.aca.2018.11.008.

[102] J.M. Moura-bueno, R. Simão, D. Dalmolin, A. Carnieletto, J.A.M. Demattê, Stratification of a local VIS-NIR-SWIR spectral library by homogeneity criteria yields more accurate soil organic carbon predictions, Geoderma 337 (2019) 565–581. https://doi.org/10.1016/j.geoderma.2018.10.015.

[103] S. Zhang, X. Lu, Y. Zhang, G. Nie, Y. Li, Estimation of soil organic matter , total nitrogen and total carbon in sustainable coastal wetlands, Sustainability (2019). https://doi.org/10.3390/su11030667.

[104] J.M. Amigo, J. Cruz, M. Bautista, S. Maspoch, J. Coello, M. Blanco, Study of pharmaceutical samples by NIR chemical-image and multivariate analysis, Trends in Analytical Chemistry 27 (2008). https://doi.org/10.1016/j.trac.2008.05.010.

[105] A.A. Gowen, C.P. O'Donnell, P.J. Cullen, S.E.J. Bell, Recent applications of chemical imaging to pharmaceutical process monitoring and quality control, European Journal of

Pharmaceutics and Biopharmaceutics 69 (2008) 10−22. https://doi.org/10.1016/j.ejpb.2007.10.013.

[106] C. Gendrin, Y. Roggo, C. Collet, Pharmaceutical applications of vibrational chemical imaging and chemometrics: a review, Journal of Pharmaceutical and Biomedical Analysis 48 (2008) 533−553. https://doi.org/10.1016/j.jpba.2008.08.014.

[107] M. Khorasani, J.M. Amigo, C.C. Sun, P. Bertelsen, J. Rantanen, Near-infrared chemical imaging (NIR-CI) as a process monitoring solution for a production line of roll compaction and tableting, European Journal of Pharmaceutics and Biopharmaceutics 93 (2015). https://doi.org/10.1016/j.ejpb.2015.04.008.

[108] J.X.J.X. Wu, J.M. Amigo, M. Bautista, J. Manuel, Moving to fast chemical imaging techniques in process control, European Pharmaceutical Review 21 (2016) 48−51.

[109] M. Khorasani, J.M. Amigo, J. Sonnergaard, P. Olsen, P. Bertelsen, J. Rantanen, Visualization and prediction of porosity in roller compacted ribbons with near-infrared chemical imaging (NIR-CI), Journal of Pharmaceutical and Biomedical Analysis 109 (2015) 11−17. https://doi.org/10.1016/j.jpba.2015.02.008.

[110] M. Khorasani, J.M. Amigo, P. Bertelsen, C.C. Sun, J. Rantanen, Process optimization of dry granulation based tableting line: extracting physical material characteristics from granules, ribbons and tablets using near-IR (NIR) spectroscopic measurement, Powder Technology 300 (2016) 120−125.